Journal of Alloys and Compounds 488 (2009) 320–324

Contents lists available at ScienceDirect

Journal of Alloys and Compounds

journal homepage: www.elsevier.com/locate/jallcom

Facile synthesis of mesoporous $ZnAl_2O_4$ thin films through the evaporation-induced self-assembly method

Xiqiang Tian[a,b], Lijuan Wan[a], Kai Pan[a], Chungui Tian[a], Honggang Fu[a,*], Keying Shi[a]

[a] Key Laboratory of Functional Inorganic Material Chemistry, Ministry of Education of the People's Republic of China, Heilongjiang University, Harbin 150080, PR China
[b] Department of Chemistry and Pharmaceutical Engineering, Suihua College, Suihua 152061, PR China

ARTICLE INFO

Article history:
Received 23 June 2008
Received in revised form 25 August 2009
Accepted 26 August 2009
Available online 31 August 2009

Keywords:
Evaporation-induced self-assembly
Triblock copolymer
Mesoporous zinc aluminate
Thin films

ABSTRACT

Mesoporous $ZnAl_2O_4$ thin films have been successfully synthesized using aluminum chloride and zinc chloride as the inorganic precursors, triblock copolymer Pluronic F-127 as the structure-directing agents, through the evaporation-induced self-assembly (EISA) method. Powder X-ray diffraction (PXRD) patterns show that the sample is single-phase cubic material with the spinel-type structure. Scanning electron microscopy (SEM) and transmission electron microscopy (TEM) were used to study the mesoporous structure of $ZnAl_2O_4$ materials. The specific surface area determined by BET surface area measurement was found to be 108.4 $m^2\ g^{-1}$. The possible formation mechanism of mesoporous $ZnAl_2O_4$ thin films was discussed.

1. Introduction

In recent years, nanostructured spinel-type complex oxides have attracted considerable attention because of their use as catalyst supports, anticorrosion pigments, as well as dielectric materials [1–4]. Among them, $ZnAl_2O_4$ represents a particularly important class of materials which have high thermal stability, high mechanical resistance, hydrophobicity, low surface acidity and wide band gap (3.8 eV) [5,6]. Due to these properties, it can be used as transparent conductor, catalysis, catalyst support, dehydration, dehydrogenation, high temperature material, polymer electrolyte and optical coating [7–15]. For the applications in catalytic field, high surface area of $ZnAl_2O_4$ is of prime importance. Generally, synthesis of nanocrystalline mesoporous $ZnAl_2O_4$ will be worthwhile to study, due to relatively higher surface area.

$ZnAl_2O_4$ is commonly synthesized by high temperature calcination of mixed zinc and aluminium oxides [16,17], or products of impregnating a porous alumina with high surface area with a solution of zinc compound [18,19]. However, the solid-state route has disadvantages as follows: lack of stoichiometry control, high temperature of reaction and lower surface area. Recently, $ZnAl_2O_4$ has been prepared through wet chemical routes such as the coprecipitated products [20,21], citric acid route [22], pechini method [23] and hydrothermal synthesis method [24]. Fine powders can by easily synthesized through these above methods. However, it is difficult to use them to prepare thin films, owing to difficulty to control the fast rate of reaction. In our previous study, we have synthesized mesoporous Al_2O_3 thin films through the evaporation-induced self-assembly (EISA) method [25,26]. The unique feature of the EISA approach is that this novel strategy combines sol–gel dip-coating and organic–inorganic cooperative assembly techniques. In our strategy, the hydrolysis velocity of inorganic species can be controlled by the interaction of hydrogen bond between H atom of $NH_3{\cdot}H_2O$ and O atom of EO in surfactant. Therefore, the inorganic precursors can hydrolyze slowly to provide relatively smaller inorganic species rather than bulk sediment. Due to the similar hydrolysis velocity of zinc salt and aluminium salt, we introduce a novel and facile route to synthesize mesoporous $ZnAl_2O_4$ thin films and powders, using aluminum chloride and zinc chloride as the inorganic precursors, triblock copolymer Pluronic F-127 as the structure-directing agents through the EISA method. As we know, mesoporous zinc aluminate thin films have little been synthesized through the facile EISA method so far. The method requires lower processing temperature and shorter heating time than conventional processing. It shows good control of stoichiometry of the particles obtained.

2. Experimental

2.1. Sample preparation

Zinc chloride (AR) and aluminium chloride (AR) were selected as starting materials for zinc and aluminum sources. Triblock copolymer Pluronic F-127 ($EO_{106}PO_{70}EO_{106}$, MW = 12600, Product No. P2443-250G) was purchased from Aldrich and used as received without further purification.

* Corresponding author. Tel.: +86 451 86608458; fax: +86 451 86673647.
E-mail address: fuhg@vip.sina.com (H. Fu).

0925-8388/$ – see front matter © 2009 Elsevier B.V. All rights reserved.
doi:10.1016/j.jallcom.2009.08.120

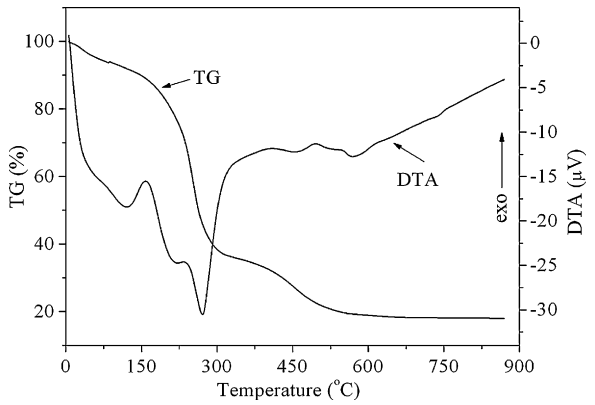

Fig. 1. TG–DTA curves of thermal decomposition of the precursor powder at the heating rate of 10 °C min^{-1} under air atmosphere.

The procedures are described in details as follows. F-127 (0.9 g) was first dissolved in ethanol (EtOH, 23 ml) at room temperature, and then $NH_3{\cdot}H_2O$ (4.5 ml) was added in the solution. The solution temperature was raised to 70 °C, and the solution was stirred constantly. After the solution composed of the surfactant, EtOH and $NH_3{\cdot}H_2O$ became clear at 70 °C, the 20 ml salts solution composed of zinc chloride (0.73 g) and aluminium chloride (2.5 g) were added in it dropwise. The solution was refluxed for 50 min at 70 °C. The final solution became clear and was cooled down. Then, they were aged for 12 h at 20–25 °C at ambient environment. The viscosity of the prepared stock solution was estimated to be 0.018 Pa S. Thin films were prepared by dip-coating silicon substrates or glass at a constant withdrawal rate (1 mm s^{-1}) and relative humidity (50–60%). Alternatively, the rest sol solutions can be dried and then calcined to prepare equivalent mesoporous $ZnAl_2O_4$ powders. The as-prepared samples were calcined at 450, 500, and 600 °C for 2 h (1 °C min^{-1} under air atmosphere). The thicknesses of the films were estimated to be about 365 ± 5 nm. Scheme 1 illustrates the experimental procedure for preparing $ZnAl_2O_4$ thin films by the EISA method.

2.2. Sample characterization

Wide-angle X-ray diffraction (XRD) patterns of the zinc aluminate powder to identify the crystalline phase were recorded on a Rigaku D/max-IIIB (40 kV, 30 mA) diffractometer, using Cu Kα radition with wavelength of λ = 1.5406 Å at room temperature. N_2-sorption isotherms of the zinc aluminate powders at 77 K were collected on a Micromeritics ASAP 2020 instrument and Brunauer–Emmett–Teller (BET) equation was used to calculate the specific surface area. Pore size distributions were obtained from the isotherm using the Barrett–Joyner–Halenda (BJH) method. Thermal behaviour of the gel precursor was studied by differential thermal analysis-thermal gravimetric (TG–DTA) using a NETZSCH STA449C thermal analyzer (10 °C min^{-1} under air atmosphere). The morphologies of mesoporous $ZnAl_2O_4$ thin films were evaluated by a Hitachi S-4800 Scanning Electron Microscope with an operating voltage of 5.0 kV. The transmission electron microscopy experiment was performed on a JEM-2100 electron microscope (JEOL, Japan) with an acceleration voltage of 200 kV. Carbon-coated copper grids were used as the sample holders. Infrared spectrum was recorded in the range 400–4000 cm^{-1} on PerkinElmer (USA) FT-IR spectrometer with KBr pellets. The film thickness was estimated by ellipsometry experiments carried out on a SENTECH GmbH/SE400 instrument with a He–Ne laser beam (λ = 632.8 nm). The viscosity of prepared stock solution were evaluated using NDJ-99 Rotating viscometer.

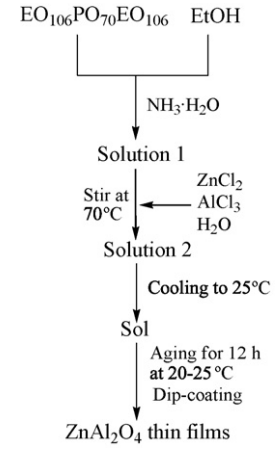

Scheme 1. Schematic diagram of the preparation of $ZnAl_2O_4$ thin films.

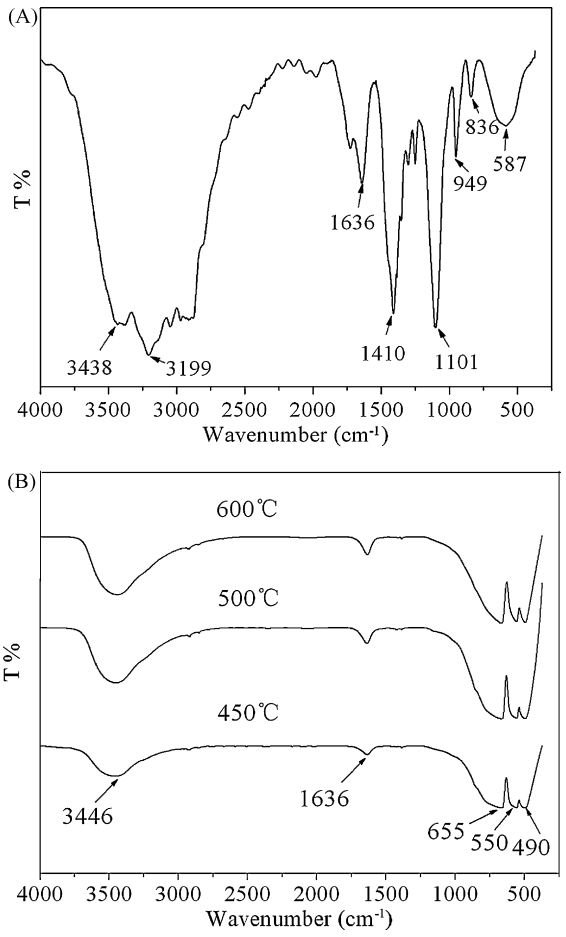

Fig. 2. IR curves of mesoporous $ZnAl_2O_4$ powder sample before (A) and after (B) calcination at 450, 500 and 600 °C for 2 h under air atmosphere, respectively.

3. Results and discussion

3.1. Thermogravemetric and differential thermal analysis

TG–DTA can provide important information about the temperature for complete removal of organic template. Fig. 1 shows the TG–DTA curves of the precursor powder samples. The TG curve shows three steps and a total weight loss of ca. 80%. The first step of ca. 15% from 20 to 180 °C could be attributed to the removal of alcohol, physisorption and interlayer water. The second significant weight loss of ca. 50% between 180 and 350 °C was assigned to the decomposition of the F127 template partly. From 350 to 500 °C, there was a weight loss of ca. 15%, which was assigned to the complete removal of residual organic template. From DTA curves we can clearly see three main endothermic peaks, which were corresponding to the weight loss of the three steps. These results show that the organic template was removable completely upon calcination at 500 °C. Above 500 °C, there was no further weight loss, which indicated that the organic component had been entirely removed.

3.2. Infrared spectroscopy

IR spectra for powder sample without calcination (A) and calcined sample at 450 °C, 500 °C, and 600 °C (B) are shown in Fig. 2.

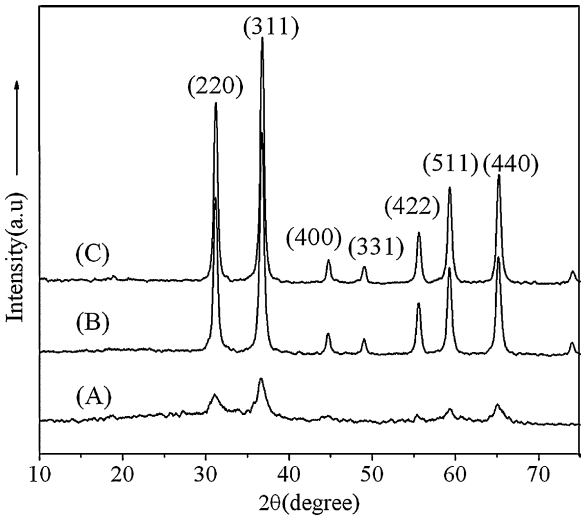

Fig. 3. XRD patterns of powder sample heat-treated for 2 h at different temperatures: (A) 450 °C; (B) 500 °C; (C) 600 °C.

Fig. 2A shows the IR spectra of the sample without calcination. The IR peaks around 1410 and 1101 cm^{-1} can be assigned to the features of the stretching vibration mode of C=O. The strong absorption peak at about 3199 cm^{-1} is corresponding to the vibration modes of metal attached hydroxy groups [27]. The peaks at around 3438 cm^{-1} and 1636 cm^{-1} were ascribed to H_2O stretching vibration bands (Fig. 2A). In addition, the peaks at 949, 836 and 587 cm^{-1} observed in Fig. 2A can be attributed to the inorganic network [28]. When the samples were calcined at 450 °C, 500 °C, 600 °C, new absorption peaks located at 655, 550 and 490 cm^{-1} are characteristic of the regular spinel structure. The IR spectra of the calcined samples are similar to that of the sample without calcination. The peaks (Fig. 2B) located below 1000 cm^{-1} correspond to AlO_6 groups, indicating the formation of $ZnAl_2O_4$ [29]. The high surface area of the calcined sample results in rapid adsorption of water from the air atmosphere, thus, the absorption peaks of H_2O can also be observed in the IR spectrum (Fig. 2B). No carbon stretching vibration peaks are observed from the FT-IR spectrum of the calcined sample (Fig. 2B), indicating the surfactant has been removed completely.

3.3. Powder X-ray diffraction (PXRD)

The powder X-ray diffraction was used to identify the crystalline phase of the calcined samples and the results are presented in Fig. 3. Seven high-intensity Bragg diffraction peaks in the range $2\theta = 32–65°$ can be indexed as (2 2 0), (3 1 1), (4 0 0), (3 3 1), (4 2 2), (5 1 1), and (4 4 0) diffraction peaks, which show the typical patterns for cubic $ZnAl_2O_4$ (JCPDS, 82-1043). No other phases were detected in the samples heated from 450 °C to 600 °C. With increase of calcination temperature, the intensity of the diffraction peaks became more narrow and intense, which is associated with an increase in the size of the particles obtained. The average grain sizes of the powders sintered at different temperatures were determined by means of the Scherrer formula: $D = K\lambda/(\beta_c - \beta_s)\cos\theta$, where λ is the wavelength of the X-ray radiation, D is the crystal size, and β_c, β_s are the full widths at half-maximum height of the sample and standard (single-crystal silicon) respectively. As calculated from the Scherrer equation using the (3 1 1) diffraction peak of mesoporous $ZnAl_2O_4$ for samples calcined at 450 °C, 500 °C and 600 °C, the average crystallite size was estimated to be 5, 18.3, and 20 nm, respectively.

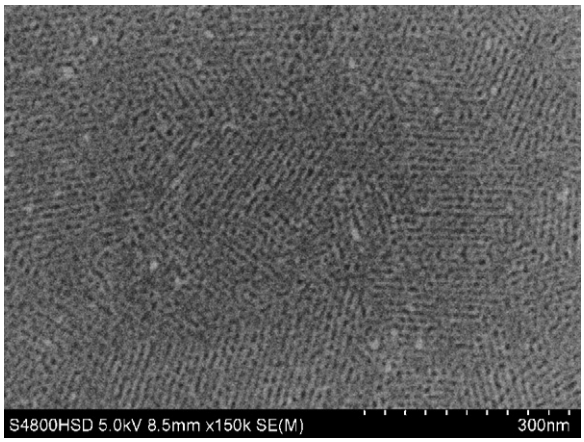

Fig. 4. Representative SEM image of the mesoporous $ZnAl_2O_4$ thin films calcined at 600 °C for 2 h under air atmosphere.

3.4. Morphology observation

Scanning electron microscopy (SEM) image of mesoporous $ZnAl_2O_4$ thin film was shown in Fig. 4. SEM image showed our obtained products possessed mesoporous structure with uniform pore size about 4 nm. Evidently, our proposed the EISA synthetic strategy is simple, which permits the synthesis of uniform mesoporous $ZnAl_2O_4$ thin films using aluminum chloride and zinc chloride as inorganic precursors and F-127 as structure-directing agent.

In order to further investigate the morphology of mesoporous $ZnAl_2O_4$, transmission electron microscopy (TEM) characterization was performed and the result was shown in Fig. 5. Unordered mesoporous structure can be clearly observed and the main pore size was about 4 nm. The TEM observation was consistent very well with the SEM results.

3.5. Determination of surface area

In order to further characterize mesoporous structure of zinc aluminate thin films, nitrogen adsorption–desorption measure-

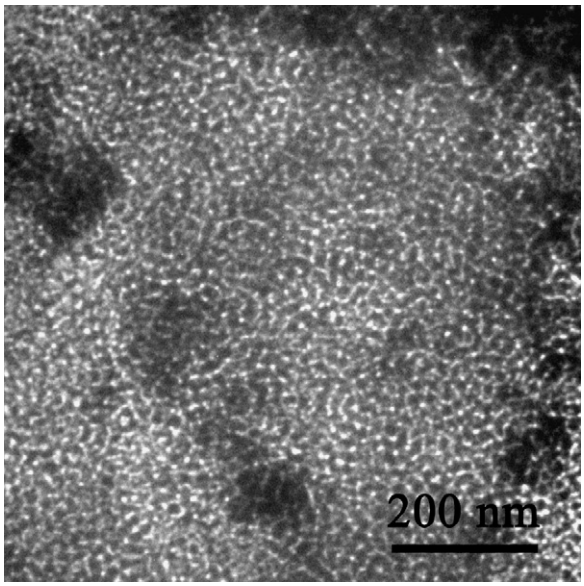

Fig. 5. TEM image of mesoporous $ZnAl_2O_4$ powders calcined at 600 °C for 2 h under air atmosphere.

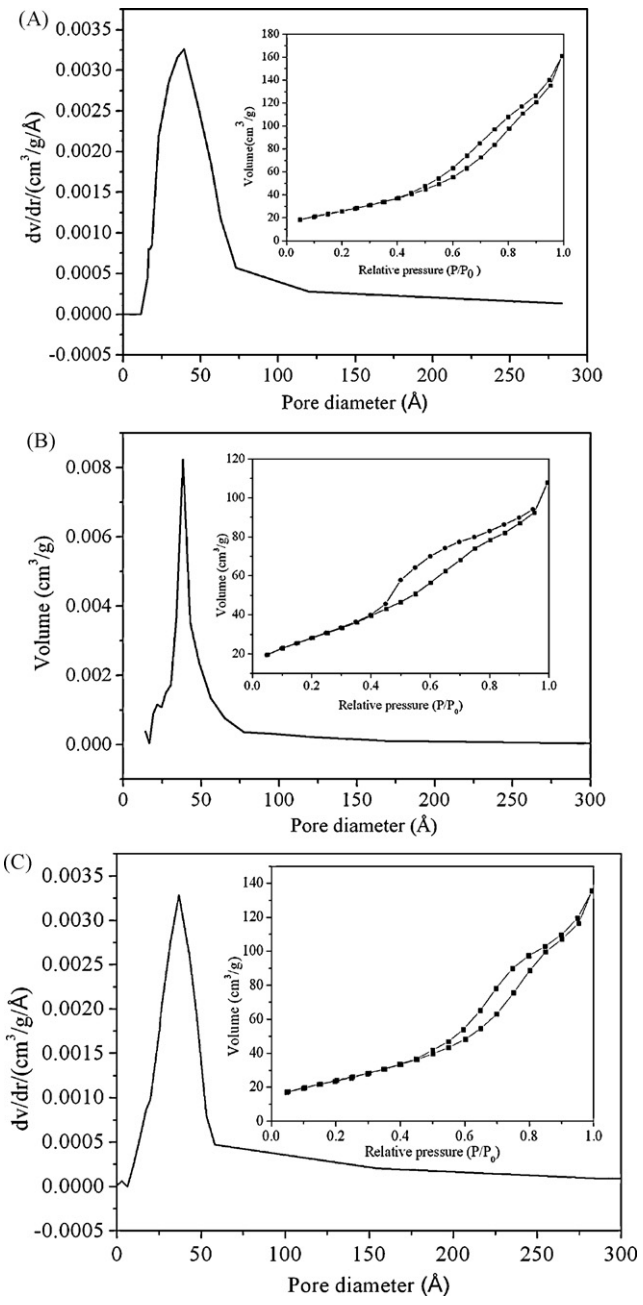

Fig. 6. N_2-sorption isotherms (inset) and corresponding pore size distribution for the sample calcined at different temperatures: (A) 450 °C; (B) 500 °C; (C) 600 °C.

ment was performed. Fig. 6 shows the N_2 adsorption–desorption isotherms for mesoporous $ZnAl_2O_4$ samples with different calcined temperature at 450, 500 and 600 °C for 2 h in air. The isotherms are typical of type-IV isotherms (according to IUPAC classification) with H3 type hysteresis loop, which is characteristic of inorganic porous oxides. The pore size distribution curves were obtained according to the Barrett–Joyner–Halenda (BJH) method, which are shown in Fig. 6. The pore size distribution curves (Fig. 6A–C) imply that pore sizes of the calcined samples are 4.0 nm, 3.8 nm and 3.7 nm, respectively. The BET surface area (S_{BET}) of the samples was gained by BET formula. The S_{BET} of $ZnAl_2O_4$ powders with calcined temperature at 450, 500 and 600 °C are 108.4, 105.2 and 98.6 $m^2\,g^{-1}$, respectively. This implies that our obtained mesoporous $ZnAl_2O_4$ materials possess of high surface area (Fig. 6).

4. Formation mechanism

The formation of mesoporous $ZnAl_2O_4$ can be attributed to the interaction between the structure-directing agent (F-127) and the hydrophilic aluminium–zinc nanoclusters and the formation of a surfactant–nanocluster hybrid. In our experiment, the $NH_3{\cdot}H_2O$ first dispersed in the surfactant solution, the hydrogen bond may be formed between the O atom of hydrophilic block and the H atom of $NH_3{\cdot}H_2O$. Hence, the reason for the slow hydrolysis velocity of inorganic species is that the interaction of hydrogen bond between the H atom of the $NH_3{\cdot}H_2O$ and the O atom of EO of the surfactant, which controls the ionization rate of $NH_3{\cdot}H_2O$ and prevent formation of bulk precipitation [25]. The zinc and aluminum precursors can hydrolyze slowly to provide relatively smaller inorganic particles rather than bulk sediment, which may have strong interaction with surfactant micelles. Such zinc–aluminum oxo-clusters can realize the assembly with surfactant. This allows for the synthesis of mesoporous $ZnAl_2O_4$ thin films via the zinc–aluminum oxo-clusters' assembling with the surfactant and prevent the pores from collapsing when the surfactant was removed. We choose proper quantity of $NH_3{\cdot}H_2O$ according to the phenomena of experiments. Only when the solution of surfactant and $NH_3{\cdot}H_2O$ became clear, a certain amount of zinc salt and aluminium salt solution could be added in it dropwise. If $NH_3{\cdot}H_2O$ was added at the last step, the product was bulk sediment. Finally, when the solution became clear, the sol was aged for several hours at 20–25 °C at ambient environment. With the evaporation of the volatile solvent, the homogeneous sol with stable mesophases could be got, the assembly of the surfactant with the inorganic species and the further cross-link of the inorganic precursors result in the final formation $ZnAl_2O_4$ with mesoporous structure.

In this technique, the assembly of organic surfactant template departs from the condensation of inorganic species, and then, with the evaporation of volatile solvents, the micelles assemble to stable mesophases. There have many advantages such as homogenous mixing of the components on an atomic scale, good control of the stoichiometry and easily operation. Referring to the molar ratio Zn:Al = 1:2, the following equation represents a probable course of the formation of $ZnAl_2O_4$.

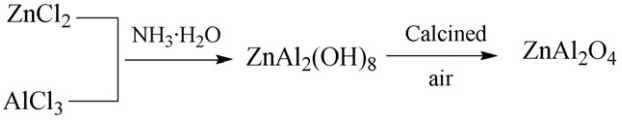

5. Conclusions

In summary, nanocrystalline mesoporous $ZnAl_2O_4$ thin films and powders have been synthesized from the combination of inexpensive and commercially available polymer and aluminum salts and zinc salts through the EISA method. The precursor calcined at 450, 500, 600 °C for 2 h in air atmosphere yields single-phase $ZnAl_2O_4$ with mesoporous structure. The $ZnAl_2O_4$ possesses of uniform pore size distribution and high specific surface area indicates that mesoporous $ZnAl_2O_4$ is a promising candidates for potential applications in catalysis, catalyst support and etc. Moreover, we have demonstrated that the hydrolysis rate of the inorganic species can be effectively controlled using this route which may be used for synthesis of other mesoporous aluminate spinels, e.g. $CoAl_2O_4$.

Acknowledgements

This work was supported by the Key Program Projects of National Natural Science Foundation of China (project no. 20431030), the National Natural Science Foundation of China

(nos. 20671032 and 20676027), and the Key Program Projects of Heilongjiang Province Natural Science Foundation of China (no. ZJG0602-01).

References

[1] W. Lei, W.Z. Lu, J.H. Zhu, X. Ye, Ceram. Int. 35 (2009) 277–280.
[2] M.A. Valenzuela, J.-P. Jacobs, P. Bosch, S. Reijne, B. Zapata, H.H. Brongersma, Appl. Catal. A: Gen. 148 (1997) 315–324.
[3] M. Nilsson, K. Jansson, P. Jozsa, L.J. Pettersson, Appl. Catal. B: Environ. 86 (2009) 18–26.
[4] D. Veselý, A. Kalendova, Prog. Org. Coat. 62 (2008) 5–20.
[5] M. Zawadzki, J. Wrzyszcz, Mater. Res. Bull. 35 (2000) 109–114.
[6] X.Y. Chen, C. Ma, Z.J. Zhang, B.N. Wang, Mater. Sci. Eng. B 151 (2008) 224–230.
[7] R. Pandey, J.D. Gale, S.K. Sampath, J.M. Recio, J. Am. Ceram. Soc. 82 (1999) 3337–3341.
[8] S.K. Sampath, J.F. Cordaro, J. Am. Ceram. Soc. 81 (1998) 649–654.
[9] A.E. Galetti, M.F. Gomez, L.A. Arrúa, M.C. Abello, Appl. Catal. A: Gen. 348 (2008) 94–102.
[10] L.M. Chen, X.M. Sun, Y.N. Liu, K.B. Zhou, Y.D. Li, J. Alloys Compd. 376 (2004) 257–261.
[11] W.S. Tzing, W.H. Tuan, J. Mater. Sci. Lett. 15 (1996) 1395–1396.
[12] M.C. Marion, E. Garbowski, M. Primet, J. Chem. Soc. Faraday Trans. 11 (1991) 1795–1800.
[13] L. Zou, X. Xiang, M. Wei, L. Yang, F. Li, D.G. Evans, Ind. Eng. Chem. Res. 47 (2008) 1495–1500.
[14] N. Guilhaume, M. Primet, J. Chem. Soc. Faraday Trans. 11 (1994) 1541–1545.
[15] M. Zawadzki, W. Mista, L. Kepinski, Vacuum 63 (2001) 291–296.
[16] W.-S. Hong, L.C. De Jonghe, X. Yang, M.N. Rahaman, J. Am. Ceram. Soc. 78 (1995) 3217–3224.
[17] K. Sampath, F. Cordaro, J. Am. Ceram. Soc. 81 (1998) 649–654.
[18] G.B. Carrier, Process for producing porous spinel materials, U.S. Patent 4, 256, 722 (1981).
[19] D.W. Walker, Zinc aluminate prepared using an alumina hydrate, U.S. Patent 4, 370, 310 (1983).
[20] G. Aguilar-Rios, M. Valenzuela, P. Salas, H. Armendariz, P. Bosch, G. Del Toro, R. Silva, V. Bertin, S. Castillo, A. Ramirez-Solis, I. Schifter, Appl. Catal. A: Gen. 127 (1995) 65–75.
[21] Y.Q. Sun, Y.M. Zhou, Z.Q. Wang, X.Y. Ye, Appl. Surf. Sci. 255 (2009) 6372–6377.
[22] X.L. Duan, D.R. Yuan, Z.H. Sun, C.N. Luan, D.Y. Pan, D. Xu, M.K. Lv, J. Alloys Compd. 386 (2005) 311–314.
[23] L. Gama, M.A. Ribeiro, B.S. Barros, R.H.A. Kiminami, I.T. Weber, A.C.F.M. Costa, J. Alloys Compd. 483 (2009) 453–455.
[24] J. Wrzyszcz, M. Zawadzki, J. Trawczyński, H. Grabowska, W. Mišta, Appl. Catal. A: Gen. 210 (2001) 263–269.
[25] L.J. Wan, H.G. Fu, K.Y. Shi, X.Q. Tian, Microporous Mesoporous Mater. 115 (2008) 301–307.
[26] L.J. Wan, H.G. Fu, K.Y. Shi, X.Q. Tian, Mater. Lett. 62 (2008) 1525–1527.
[27] C.C. Yang, S.Y. Chen, S.Y. Cheng, Powder Technol. 148 (2004) 3–6.
[28] J. Parmentier, M. Richard-Plouet, S. Vilminot, Mater. Res. Bull. 33 (1998) 1719–1720.
[29] X.H. Wei, D.H. Chen, Mater. Lett. 60 (2006) 823–827.